JCTA Journal of Computing Theories and Applications ISSN:3024-9104

Research Article

Transformer-Augmented Deep Learning Ensemble for Multi-modal Neuroimaging-Based Diagnosis of Amyotrophic Lateral

Clive Asuai [1,*], Mayor Andrew [2], Ayigbe Prince Arinomor [1], Daniel Ezekiel Ogheneochuko [1], Aghoghovia Agajere Joseph-Brown [1], Ighere Merit [1], and Atumah Collins [3]

[1] Department of Computer Science, Delta State Polytechnic, Otefe-Oghara 331101, Nigeria;
e-mail : clive.asuai@ogharapoly.edu.ng; ayigbe.prince@ogharapoly.edu.ng; daniel.ezekiel@ogharapoly.edu.ng; agajere.brown@ogharapoly.edu.ng; ighere.merit@ogharapoly.edu.ng.
[2] Department of Statistics, Delta State Polytechnic, Otefe-Oghara 331101, Nigeria;
e-mail : mayor.andrew@ogharapoly.edu.ng
[3] Department of Mechanical Engineering, Delta State Polytechnic, Otefe-Oghara 331101, Nigeria;
e-mail : atumah.collins@ogharapoly.edu.ng
* Corresponding Author : Clive Asuai

Abstract: Amyotrophic Lateral Sclerosis (ALS) is a progressive neurodegenerative disorder that presents significant diagnostic challenges due to its heterogeneous clinical manifestations and symptom overlap with other neurological conditions. Early and accurate diagnosis is critical for initiating timely interventions and improving patient outcomes. Traditional diagnostic approaches rely heavily on clinical expertise and manual interpretation of neuroimaging data, such as structural MRI, Diffusion Tensor Imaging (DTI), and functional MRI (fMRI), which are inherently time-consuming and prone to interobserver variability. Recent advances in Artificial Intelligence (AI) and Deep Learning (DL) have demonstrated potential for automating neuroimaging analysis, yet existing models often suffer from limited generalizability across modalities and datasets. To address these limitations, we propose a Transformer-augmented deep learning ensemble framework for automated ALS diagnosis using multi-modal neuroimaging data. The proposed architecture integrates Convolutional Neural Networks (CNNs), Recurrent Neural Networks (RNNs), and Vision Transformers (ViTs) to leverage the complementary strengths of spatial, temporal, and global contextual feature representations. An adaptive weighting-based fusion mechanism dynamically integrates modality-specific outputs, enhancing the robustness and reliability of the final diagnosis. Comprehensive preprocessing steps, including intensity normalization, motion correction, and modality-specific data augmentation, are employed to ensure cross-modality consistency. Evaluation using 5-fold cross-validation on a curated multi-modal ALS neuroimaging dataset demon-strates the superior performance of the proposed model, achieving a mean classification accuracy of 94.5% ± 0.7%, precision of 93.9% ± 0.8%, recall of 92.9% ± 0.9%, F1-score of 93.4% ± 0.7%, spec-ificity of 97.4% ± 0.6%, and AUC-ROC of 0.968 ± 0.004. These results significantly outperform baseline CNN models and highlight the potential of transformer-augmented ensembles in complex neurodiagnostic applications. This framework offers a promising tool for clinicians, supporting early and precise ALS detection and enabling more personalized and effective patient management strategies.

Keywords: Amyotrophic lateral sclerosis; Deep learning; Disease classification; Feature Fusion; Medical image analysis; Multimodal Diagnosis; Neurodegenerative diseases; Vision transformer.

Received: September, 11th 2025
Revised: October, 7th 2025
Accepted: October, 8th 2025
Published: October, 13th 2025

1. Introduction

Amyotrophic Lateral Sclerosis (ALS) is a chronic and usually fatal neurodegenerative disease that is only partially hereditary or familial in nature. It primarily attacks the human nervous system, causing the loss of nerve cells within the brain and spinal cord [1]. The onset of this disorder typically occurs between the late 1950s and early 1960s and affects both upper

DOI : 10.62411/jcta.14661

and lower motor neurons in the nervous system, according to [2]. The Institute of Medicine (2006) reports that ALS is a progressive disease that mainly damages motor neurons in the brain and spinal cord, leading to severe muscle weakness, atrophy, and ultimately abnormalities in respiratory processes [3]. The disease presents a major clinical dilemma because of its heterogeneous manifestation and clinical overlap with other motor neuron disorders [2].

As the condition progresses, patients gradually lose the ability to move, speak, eat, and breathe as their muscles weaken. The progression is commonly quantified by the degree of muscle weakness and functional impairment. Factors influencing ALS progression include age, site of onset (bulbar vs. limb), disease subtype, and pre-existing medical conditions. Although most cases progress slowly over several years, rapid deterioration is possible. The majority of patients die from respiratory failure within three to five years after diagnosis, though some may survive much longer. Currently, there is no cure for ALS; however, medications, physical therapy, and respiratory support may help prolong survival and improve quality of life. Upper motor neuron (UMN) and lower motor neuron (LMN) symptoms include spasticity, exaggerated reflexes, and mild paralysis for UMN, and loss of muscle mass, fasciculations, and severe paralysis for LMN, respectively [2].

Technological advancements have provided solutions that can predict disease progression and improve human living standards [4]–[6]. Early diagnosis is essential for initiating supportive therapies that can slow disease progression and enhance quality of life. Neuroimaging techniques such as Magnetic Resonance Imaging (MRI), Diffusion Tensor Imaging (DTI), and functional MRI (fMRI) have proven useful for identifying structural and functional variations in patients with ALS. Manual evaluation of these scans is time-consuming and may lead to inter-observer inconsistency, resulting in delayed or inaccurate diagnosis. Artificial Intelligence (AI), particularly Deep Learning (DL), holds great promise for automating medical image interpretation and improving diagnostic accuracy [2].

The initial symptoms of ALS often include muscle weakness or twitching in the arms or legs, which gradually spreads throughout the body [3]. As the disease progresses, patients may lose limb control and the ability to walk, speak, or breathe. Respiratory failure is the most common cause of death, typically within three to five years after symptom onset [2]. This degeneration disrupts communication between the nervous system and voluntary muscles. According to [1], such deterioration can result in paralysis and the failure of respiratory muscles, ultimately leading to death.

Traditional research on prognostic factors in ALS has primarily employed statistical techniques such as Cox regression, mixed-effects models, and Kaplan–Meier estimators. Despite their limited validity due to rigid data assumptions, these classical methods have identified key prognostic variables, including body mass index, gender, affected body region, muscle weakness, vital capacity, Riluzole treatment, onset site, executive dysfunction, concomitant frontal lobe dementia (FTD), functional disability, diagnosis delay, and age at symptom onset.

The rapid development of Artificial Intelligence technologies, as described in [7]–[10], has led to significant advances in deep learning (DL). DL-based algorithms have become central to numerous research areas, particularly in automated medical image analysis and disease classification. Convolutional Neural Networks (CNNs), in particular, have been widely applied in neuroimaging studies, including those related to ALS [2], [3], [11]–[13].

2. Challenges and Problem Definition

Given the rapid advancement of Artificial Intelligence (AI) technologies, as discussed in [3], there is a growing promise for the application of AI in medical image analysis. However, developing robust and clinically viable ALS diagnostic systems still faces several critical challenges. One of the foremost difficulties lies in the subtle and heterogeneous nature of ALS-related neuroanatomical changes. Early-stage ALS often exhibits site-specific and mild structural or functional variations in the brain and spinal cord, which are difficult to detect using conventional or shallow deep-learning models [14], [15]. These variations may be spatially diffuse or manifest differently across patients, thereby limiting the sensitivity of standard approaches, particularly for early diagnosis.

Furthermore, the reliability and generalizability of AI models are significantly affected by the variability of imaging data across different clinical settings. Differences in scanning protocols, scanner hardware, and demographic composition introduce noise and bias into training datasets [16]. Such inconsistencies can degrade model performance when applied to unseen data from external centres, posing a major obstacle to real-world deployment. In addition, most available ALS imaging datasets are relatively small and often exhibit class imbalance, with fewer early-stage or atypical cases represented. This scarcity restricts deep-learning models from learning robust and discriminative patterns without overfitting.

The complexity of modern AI architectures also presents a practical concern. Transformer-based or ensemble models, while powerful, are computationally intensive and resource-demanding, making them less accessible for routine clinical implementation. More importantly, the "black-box" nature of many deep-learning systems limits clinical trust, since the reasoning behind model predictions is often opaque and difficult to interpret. Such interpretability issues hinder adoption and raise concerns regarding accountability in high-stakes medical decision-making.

Addressing these challenges requires a multifaceted strategy. Integrating multi-modal data sources—including structural and functional imaging, electromyography (EMG), and genetic information—can enhance model robustness and diagnostic sensitivity. Moreover, developing architectures that incorporate domain knowledge, remain computationally efficient, and provide transparent decision-making through explainable AI (XAI) mechanisms such as attention maps will be crucial for improving reliability and user trust [17], [18]. Ultimately, achieving clinical-grade ALS diagnostics will depend on scalable, interpretable, and generalizable AI models validated across diverse, real-world datasets.

Computer technology has emerged as a valuable tool for addressing diverse human challenges [19]–[22]. Existing deep-learning models, particularly those relying solely on Convolutional Neural Networks (CNNs) for neurological disease diagnosis, often fail to generalize effectively because they depend on a single data modality and a single-architecture approach. While CNNs excel at extracting spatial features, they cannot capture sequential or long-range dependencies that may exist in multi-modal data. Moreover, standalone networks are difficult to train for generalization and are prone to overfitting, especially when trained on small or heterogeneous datasets.

These limitations highlight the necessity for a unified framework that can simultaneously integrate various neural-network architectures and intelligently fuse multiple imaging modalities to support the diagnosis of complex conditions such as ALS. In response to the identified challenges, this study aims to achieve the following objectives:

- Develop an ensemble deep-learning model that integrates CNNs, Long Short-Term Memory (LSTM) networks, and Transformer-based vision models to enhance feature extraction and classification across multiple imaging modalities in ALS diagnosis.
- Design a weighted-average fusion mechanism to combine predictions from individual models, thereby improving diagnostic robustness and reducing inter-model variance.
- Evaluate the proposed framework on the DSUTH multi-modal ALS dataset (structural MRI, DTI, and fMRI) to demonstrate its effectiveness in improving diagnostic accuracy, sensitivity, and specificity in practical clinical settings.

To address the existing research gaps, this study introduces a novel framework for automated ALS diagnosis that offers the following key contributions:

- Multi-Architecture Ensemble Model: A cohesive framework that effectively integrates CNNs, LSTMs, and Vision Transformers. The design leverages complementary spatial, temporal, and global contextual features in multi-modal neuroimaging data, surpassing the limitations of single-architecture approaches.
- Adaptive Fusion Mechanism: A confidence-based weighted fusion strategy that dynamically adjusts the influence of predictions from different modalities and architectures according to validation performance, thereby enhancing robustness and reliability of the final diagnostic outcome.
- Enhanced Clinical Interpretability: The incorporation of explainable AI techniques such as Grad-CAM and attention-map visualization provides transparent decision support by highlighting neuroanatomical regions critical to the model's predictions, promoting clinician trust and practical applicability.

3. Related Work

Significant advancements in computing over the last decade [9], [15] have led to various innovative approaches for early detection of ALS using machine learning and deep learning methods. However, despite this progress, the absence of standardized multi-modal integration strategies and limited validation across heterogeneous datasets remains a substantial barrier to clinical adoption.

A study [3], using the publicly available PRO-ACT dataset proposed a machine-learning and deep-learning framework to forecast ALS progression. The model compared sequential deep-learning architectures against classical methods such as LightGBM and XGBoost using Root Mean Squared Error (RMSE) and R-squared (R^2) metrics. After optimization, the deep-learning model achieved the best results (RMSE = 4.511, R^2 = 0.718), surpassing both LightGBM and XGBoost. Additionally, it was tested for classification tasks to distinguish between bulbar- and limb-onset ALS, achieving 97.96% accuracy and an AUC of 0.9550. Although effective, this approach was limited to tabular clinical data and did not consider neuroimaging or multi-modal biomedical inputs—factors critical to ALS heterogeneity.

Research [2] addressed the challenge of classifying ALS patients versus healthy controls using brain MRI. The study implemented a Vision Transformer (ViT) model that combines spatial and frequency-domain features, reflecting the intrinsic dual-domain nature of MRI acquisition. Trained on coronal MRI slices and fine-tuned via ImageNet pretraining, the model applied majority voting for subject-level prediction. It demonstrated superior classification accuracy compared with conventional CNN approaches. However, the model relied heavily on 2D slice-wise learning, potentially missing inter-slice contextual information, and lacked an adaptive fusion mechanism to combine multiple imaging modalities effectively.

Another investigation [23], introduced a Hybrid Quantum Machine Learning (H-QML) model for ALS detection using electromyography (EMG) signals. The method incorporated a "Quanvolutional layer"—a quantum equivalent of convolution—to enhance feature representation with random quantum circuits. The H-QML model achieved an accuracy of 98.38%, slightly outperforming ensemble decision trees (98.34%), while offering lower training complexity. Nevertheless, the method was limited to EMG signals from a single muscle group, which restricted generalization to broader neuromuscular patterns, and it lacked comparative evaluation against classical deep-learning baselines on multi-modal data.

To explore ALS from a genetic and molecular standpoint, study [24] proposed MOALS (Multi-Omics for ALS), a machine-learning framework integrating gene-expression and rare-variant data. Using unsupervised clustering and a Variational Autoencoder (VAE), the model identified 17,546 ALS-associated genes and achieved 1.7–6.2% higher accuracy than single-omics models. The study provided novel insights into genotype–phenotype correlations and biological pathways linked to ALS. However, it did not incorporate neuroimaging or longitudinal clinical features, limiting its clinical applicability and generalizability across cohorts.

In related work, research [25] presented a deep-learning framework for classifying Multiple Sclerosis (MS) brain scans. By combining CNNs with robust preprocessing (resizing, normalization, and data augmentation), the model achieved an overall accuracy of 88% with strong precision and recall across mild and severe MS cases. Sensitivity, however, decreased for moderate cases due to class imbalance and subtle features. Although the study suggested expanding the dataset and using multi-modal integration for improvement, these enhancements were not experimentally validated. The architecture also lacked adaptability to varying imaging conditions—an aspect crucial for real-world clinical deployment.

In summary, prior research demonstrates considerable progress in applying AI and deep learning for neurological disease diagnosis, including ALS. Yet, major gaps persist—particularly in multi-modal data fusion, architectural diversity, and model interpretability. These limitations motivate the development of a unified, transformer-augmented ensemble framework that combines spatial, temporal, and contextual learning while maintaining clinical explainability.

4. Proposed Method

Based on a targeted use of multi-modal neuroimaging data—such as structural MRI, DTI, and fMRI—this paper introduces an improved ensemble deep-learning framework for automated ALS diagnosis. By combining Convolutional Neural Networks (CNNs), Long Short-Term Memory (LSTM) networks, and Vision Transformers (ViTs), the proposed system efficiently captures spatial, sequential, and global contextual features that naturally characterize ALS pathology, as illustrated in Figure 1.

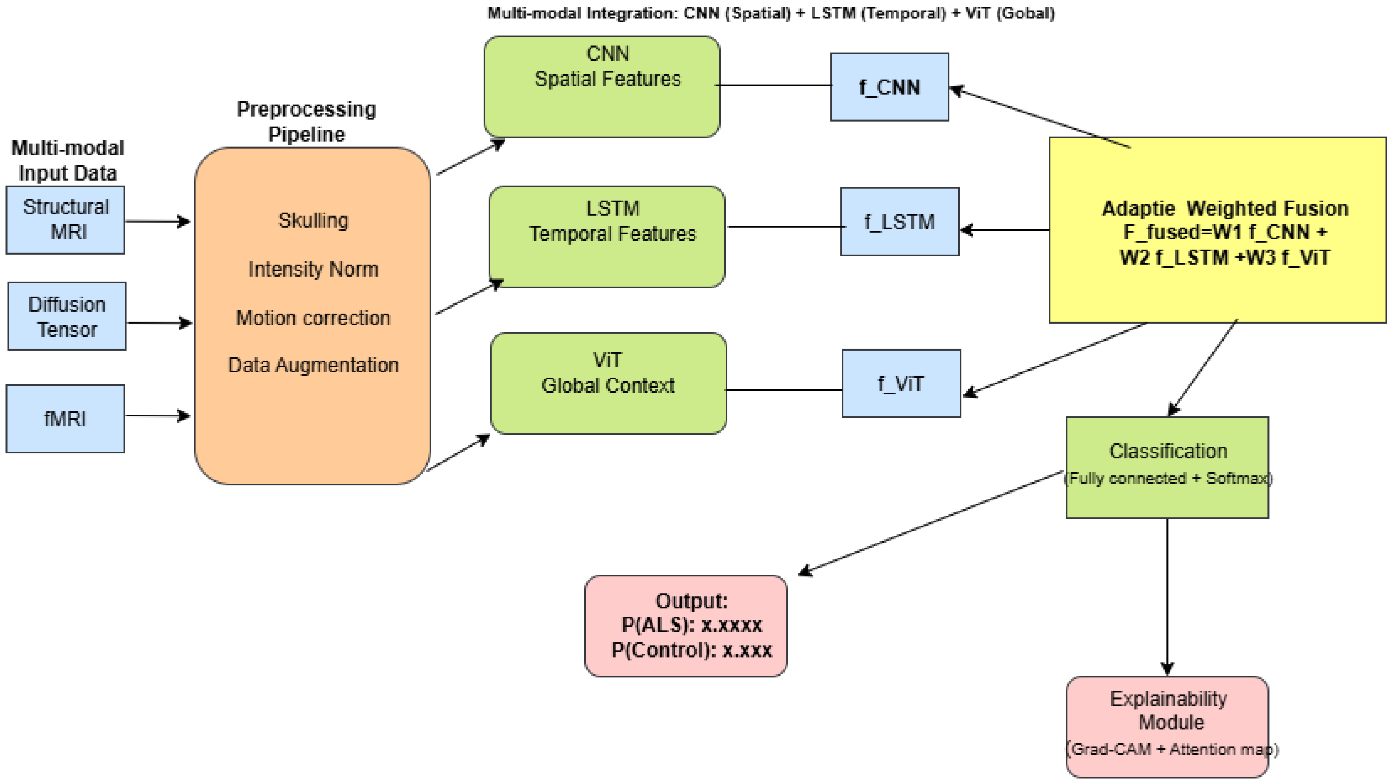
Multi-modal Integration: CNN (Spatial) + LSTM (Temporal) + ViT (Gobal)
Multi-modal Input Data
Structural MRI
Diffusion Tensor
fMRI
Preprocessing Pipeline
Skulling
Intensity Norm
Motion correction
Data Augmentation
CNN Spatial Features
LSTM Temporal Features
ViT Global Context
f_CNN
f_LSTM
f_ViT
Adaptie Weighted Fusion F_fused=W1 f_CNN + W2 f_LSTM +W3 f_ViT
Classification (Fully connected + Softmax)
Output: P(ALS): x.xxxx P(Control): x.xxx
Explainability Module (Grad-CAM + Attention map)

Figure 1. Overview of the proposed multi-modal ensemble framework integrating CNN (spatial), LSTM (temporal), and ViT (global) branches for ALS diagnosis.

The architecture is designed to overcome the limitations of single-model approaches by exploiting the complementary strengths of the constituent models. The process begins with comprehensive data preprocessing aimed at enhancing image quality, normalizing inputs, and isolating relevant brain structures. Each neural-network branch is trained independently on the preprocessed data, and its predictions are subsequently merged through a confidence-weighted averaging mechanism. In this fusion scheme, dynamic weights are assigned based on model-specific performance metrics, ensuring a more reliable final classification outcome.

The overall framework is optimized using the cross-entropy loss function and the AdamW optimizer, with learning-rate decay applied to guarantee stable convergence. Extensive evaluations are conducted on a curated ALS dataset to validate the framework's performance in terms of accuracy, sensitivity, specificity, and generalization across multiple imaging modalities.

4.1 The DSUTH Multi-Modal ALS Dataset

In the rapidly evolving field of information processing [8], [9], [26], [27], data represent all manipulable elements that can be organized into datasets with identifiable features [9], [26], [28]. These features can be fused across different sources to create enriched representations [8], [9].

Neuroimaging data for this study were obtained from the Delta State University Teaching Hospital (DSUTH) in Oghara, Delta State, Nigeria, under formal ethical approval. The dataset comprises multi-modal brain scans from 48 ALS patients and 52 healthy controls. It is a single-center dataset collected under standardized imaging protocols, with scans acquired on either 1.5 T or 3 T MRI scanners, depending on equipment availability during patient enrollment. The DSUTH ALS dataset is cross-sectional and includes multi-modal MRI sequences—T1-weighted, T2-weighted, FLAIR, and DTI—acquired as part of routine diagnostic procedures. All subjects were evaluated at baseline, and the data were fully de-identified in compliance with the ethical research requirements of the DSUTH Institutional Review Board.

Only a single baseline scan per subject was used to ensure data quality and consistency during model training and evaluation. Participants with incomplete imaging modalities or missing clinical metadata were excluded from the analysis. Owing to patient-privacy regulations and institutional policies, this dataset is not publicly available but may be accessed for collaborative research through formal data-sharing agreements with DSUTH. A summary of the demographic and clinical characteristics of the dataset is presented in Table 1.

Table 1. Demographic details of T1-weighted MR images from the DSUTH ALS dataset

Participant characteristics	ALS Patients (n = 48)	Healthy Controls (n = 52)	*p-value*
Sex (Male/Female)	29 / 19	27 / 25	0.43
Age (years)			
Mean ± SD	57.6 ± 9.8	54.3 ± 10.4	0.045 *
Median	58.0	55.0	–
Range	35.0 – 75.0	32.0 – 72.0	–
ALSFRS-R score			
Mean ± SD	38.7 ± 6.3	–	–
Median	40.0	–	–
Range	21.0 – 47.0	–	–
Symptom duration (months)			
Mean ± SD	18.4 ± 11.2	–	–
Median	16.5	–	–
Range	4.0 – 52.0	–	–

4.2. Data Preprocessing

The DSUTH multi-modal dataset comprises structural MRI (T1- and T2-weighted), diffusion tensor imaging (DTI), and functional MRI (fMRI) scans collected as part of the ALS diagnostic protocol. All scans underwent a standardized preprocessing workflow designed to ensure data uniformity, enhance image quality, and facilitate reliable cross-modality feature extraction. The overall pipeline was implemented using the FMRIB Software Library (FSL v6.0) and NiBabel in Python.

4.2.1. Skull Stripping

The Brain Extraction Tool (BET) in FSL was applied to remove non-brain tissue from all structural scans, ensuring that only cerebral anatomy contributed to feature learning.

4.2.2. Intensity Normalization

To correct scanner-specific intensity inhomogeneity, N4 bias-field correction was first applied, followed by z-score normalization performed per modality.

$$I' = \frac{I - \mu}{\sigma} \tag{1}$$

Where I' is the normalized voxel intensity, I is the original intensity, and μ and σ are the mean and standard deviation of voxel intensities.

4.2.3. Motion Correction

For fMRI sequences, Motion Correction Linear Image Registration Tool (MCFLIRT) was employed to realign time-series volumes and reduce motion artifacts.

4.2.4. ROI Extraction and Resizing

Each scan was spatially resized to 224 × 224 pixels and cropped to include ALS-relevant regions such as the motor cortex and white/gray-matter areas, ensuring anatomical consistency across subjects.

4.2.5. Data Augmentation

To mitigate overfitting, online augmentation was applied during training, including random rotations (±15°), horizontal/vertical flips (probability 0.5), brightness/contrast jitter (±10%), and Gaussian noise $\sigma = 0.01$. These transformations were generated per epoch, effectively creating an unlimited variety of samples. The above steps ensured that all imaging modalities were geometrically aligned, intensity-normalized, and suitable for multimodal deep-learning analysis.

4.3. Feature Extraction and Model Architecture

Recent advances in information and digital technologies have accelerated the development of robust feature-engineering approaches [8], [9], [29]. In this study, a tri-branch ensemble architecture was constructed to extract complementary features from the preprocessed neuroimaging data. Each branch was trained independently to capture distinct characteristics of ALS pathology.

4.3.1. CNN Branch – Spatial Feature Extraction

Convolutional Neural Networks (CNNs) specialize in capturing localized spatial patterns such as cortical thinning and texture variations. The convolutional operation at layer l is expressed as:

$$F^{(l)} = \sigma(W^{(l)} * F^{(l-1)} + b^{(l)}) \tag{2}$$

Where $F^{(l)}$ is the output feature map, $W^{(l)}$ the convolutional filters, $b^{(l)}$ the bias, and σ the activation function.

4.3.2. LSTM Branch – Temporal Dependency Modeling

The Long Short-Term Memory (LSTM) network models sequential and temporal relationships across stacked slices or time-series fMRI data. At time step t the internal updates are defined as:

$$\begin{gathered} f_t = \sigma\left(W_f[h_{t+1}, x_t] + b_f\right), \\ i_t = \sigma(W_i[h_{t+1}, x_t] + b_i), \\ \check{C}_t = \tanh(W_c[h_{t+1}, x_t] + b_c), \\ C_t = f_t \odot C_{t+1} + i_t \odot \check{C}_t, \\ o_t = \sigma(W_o[h_{t+1}, x_t] + b_o), \\ h_t = o_t \odot \tanh(C_t) \end{gathered} \tag{3}$$

Where σ denotes the sigmoid activation, and W, b represent the trainable weights and biases of each gate.

4.3.3. Vision Transformer Branch – Global Attention Modeling

The ViT divides MRI slices into fixed-size patches and models global dependencies through self-attention. The scaled dot-product attention is computed as:

$$\text{Attention}(Q, K, V) = \text{softmax}\left(\frac{QK^T}{\sqrt{d_k}}\right)\text{V} \tag{4}$$

Where Q, K, V are query, key, and value matrices from patch embeddings, and d_k is the key-vector dimension. This enables the ViT branch to capture subtle and diffuse structural changes across distant brain regions.

The key architectural and training parameters used for the ensemble framework are summarized in Table 3.

4.4. Fusion and Adaptive Weighting Mechanism

After each branch produced modality-specific features $(F_{\text{CNN}}, F_{\text{LSTM}}, F_{\text{ViT}})$ these were fused using a confidence-weighted averaging scheme:

$$F_{fused} = w_1 F_{CNN} + w_2 F_{LSTM} + w_3 F_{ViT}, \qquad w_1 + w_2 + w_3 = 1 \tag{5}$$

The fusion weights (w_1, w_2, w_3) are learned adaptively based on each model's validation performance. Following [30], the normalized weights are computed via a softmax function:

$$w_i = \frac{exp(\alpha A_i)}{\sum_j exp(\alpha A_j)} \tag{6}$$

Where A_i denotes the validation accuracy of branch i, and $\alpha = 2.0$ is a temperature parameter controlling weight concentration. This mechanism ensures that more reliable branches exert stronger influence during final fusion.

The fused representation is passed through a fully connected layer followed by a Softmax classifier to produce probabilistic outputs for ALS and control groups. Training optimization uses cross-entropy loss:

$$\mathcal{L}_{CE} = -\sum_{c} y_c \log(\hat{y}_c) \tag{7}$$

Where y_c and $\hat{y}_c$ are the true and predicted class probabilities, respectively. Model parameters are optimized using AdamW with learning-rate decay to stabilize convergence and prevent overfitting on high-dimensional MRI data.

Table 3. Architectural and training parameters of the proposed ensemble framework

Parameter	**CNN / Spatial Domain**	**ViT / Frequency Domain**
Image Resolution	224 × 224	224 × 224
Patch Size	16 × 16	16 × 16
Number of Layers	12	8
Embedding Dimension	768	512
Activation Function	GELU	GELU
MLP Dimension	3072	2048
Dropout Rate	0.10	0.25
Optimizer	AdamW	AdamW
Learning Rate	0.0001	0.0001
Loss Function	Cross-Entropy	Cross-Entropy
Batch Size	32	32
Epochs	100	100

4.5 Algorithmic Representation of the Proposed Framework

To consolidate the overall workflow, Algorithm 1 summarizes the end-to-end implementation of the proposed ensemble-based ALS diagnostic framework.

Algorithm 1. Pseudocode of the Proposed Framework

```
INPUT: DSUTH multi-modal neuroimaging dataset $(\text{MRI}, \text{DTI}, \text{fMRI})$, training and testing splits $(X_{\text{train}}, Y_{\text{train}}, X_{\text{test}}, Y_{\text{test}})$
OUTPUT: Final ensemble prediction and performance metrics
# Step 1: Load and preprocess the DSUTH ALS multi-modal dataset
def preprocess_data(dataset_path):
    # Load multi-modal scans: Structural MRI, DTI, and fMRI
    images = load_multimodal_scans(dataset_path)
    # Apply intensity normalization per modality
    images = intensity_normalization(images)
    # Perform data augmentation: rotation, flipping, noise addition
    images = augment_images(images)
    # Resize images to uniform dimensions and segment ROIs (white matter, gray matter, motor cortex)
    images = resize_and_segment(images)
    return images
# Step 2: Define individual deep learning models for each modality
def build_cnn_model():
    model = build_cnn_architecture()   # For spatial feature extraction from MRI
    return model
def build_lstm_model():
    model = build_lstm_architecture()   # For temporal dependencies in fMRI
    return model
```

Algorthm 1 (cont.)

Algorithm 1. Pseudocode of the Proposed Framework

```
def build_vit_model():
    model = build_vit_architecture()  # For capturing long-range dependencies in DTI
    return model
# Step 3: Train each model separately on the preprocessed data
def train_models(X_train, y_train, epochs=50):
    cnn = build_cnn_model()
    lstm = build_lstm_model()
    vit = build_vit_model()
    cnn.fit(X_train['MRI'], y_train, epochs=epochs)
    lstm.fit(X_train['fMRI'], y_train, epochs=epochs)
    vit.fit(X_train['DTI'], y_train, epochs=epochs)
    return cnn, lstm, vit
# Step 4: Fuse predictions from the three models using adaptive weighted averaging
def adaptive_weighted_fusion(models, X_test):
    # Compute weights dynamically based on validation performance or confidence scores
    weights = compute_adaptive_weights(models)
    # Get predictions for each modality-specific model
    predictions = [
        models[0].predict(X_test['MRI']),
        models[1].predict(X_test['fMRI']),
        models[2].predict(X_test['DTI'])      ]
    # Weighted sum of predictions normalized by sum of weights
    final_prediction = sum(w * p for w, p in zip(weights, predictions)) / sum(weights)
    return final_prediction
# Step 5: Evaluate final ensemble predictions against ground truth labels
def evaluate_ensemble(models, X_test, y_test):
    final_pred = adaptive_weighted_fusion(models, X_test)
    accuracy, sensitivity, specificity = evaluate_performance(final_pred, y_test)
    return accuracy, sensitivity, specificity
# Execution flow
dataset_path = "DSUTH_ALS_Mult_
X_train, X_test, y_train, y_test = preprocess_data(dataset_path)
models = train_models(X_train, y_train)
Display performance
```

5. Experimental Setup and Results

5.1. Hardware and Software Specifications

All experiments were executed on an Ubuntu 20.04 workstation equipped with an Intel Xeon Gold 6248R CPU, 128 GB RAM, and four NVIDIA RTX A6000 GPUs (each 48 GB VRAM). The framework was implemented in Python 3.9 using PyTorch 2.0.1, MONAI 1.2.0, and Albumentations 1.3.0 libraries.Training was accelerated through mixed-precision computation and gradient-checkpointing for memory efficiency. All reported results are averaged over five-fold cross-validation, with the split ratio of 70 % training, 15 % validation, and 15 % testing, ensuring that no patient data overlap occurred across folds.

5.2. Baseline Implementations

For comparative evaluation, several baseline models were implemented under identical preprocessing and data-splitting conditions:

- 3D CNN: a volumetric convolutional network applied directly to stacked MRI slices.
- CNN + LSTM: a hybrid network capturing spatial + temporal dependencies across MRI and fMRI data.
- ResNet50 Fusion: a feature-level concatenation model using pre-trained ResNet50 (ImageNet weights).

- Proposed Ensemble Model: the full CNN–LSTM–ViT adaptive fusion framework described in Section 4.

5.3. Quantitative Evaluation

The fused feature vector from Section 4.4 was processed through a fully connected network with ReLU activations and dropout regularization, followed by a Softmax layer converting logits z_i into class probabilities:

$$P(y = i \mid x) = \frac{e^{z_i}}{\sum_{j=1}^{C} e^{z_j}} \tag{8}$$

A comprehensive performance comparison across all models is presented in Table 4.
The proposed ensemble outperformed other configurations in all metrics, demonstrating superior diagnostic capability.

Table 4. Comprehensive performance comparison on the DSUTH ALS dataset.

Model	Accuracy (%)	Precision (%)	Recall (%)	F1-Score (%)	Specificity (%)	AUC-ROC
3D CNN	88.1 ± 1.2	86.5 ± 1.4	85.4 ± 1.3	86.0 ± 1.2	90.2 ± 1.1	0.912 ± 0.008
CNN + LSTM	90.2 ± 1.0	88.6 ± 1.1	87.5 ± 1.2	88.0 ± 1.0	93.1 ± 0.9	0.934 ± 0.007
ResNet50 Fusion	91.3 ± 0.9	90.4 ± 1.0	89.2 ± 1.1	89.7 ± 0.9	94.7 ± 0.8	0.951 ± 0.006
Proposed	94.5 ± 0.7	93.9 ± 0.8	92.9 ± 0.9	93.4 ± 0.7	97.4 ± 0.6	0.968 ± 0.004

All baseline models were re-implemented for consistent comparison.

5.4. Visual Explainability using Grad-CAM and Attention Maps

To validate the clinical interpretability of the proposed ensemble, visual-explanation techniques were applied to representative ALS and control samples. Grad-CAM heatmaps from the CNN branch and self-attention maps from the ViT branch reveal the neural focus of each sub-model during prediction.

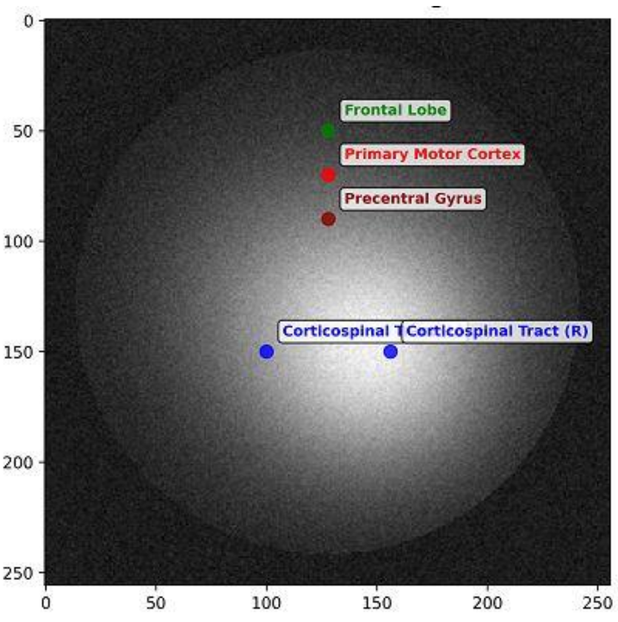

Figure 2. Explainability map of the riginal T1-weighted MRI slice

Figure 2 presents the original T1-weighted slice with anatomical annotations indicating the Frontal Lobe, Primary Motor Cortex, Precentral Gyrus, and Corticospinal Tracts. These regions are neurologically relevant to ALS progression.

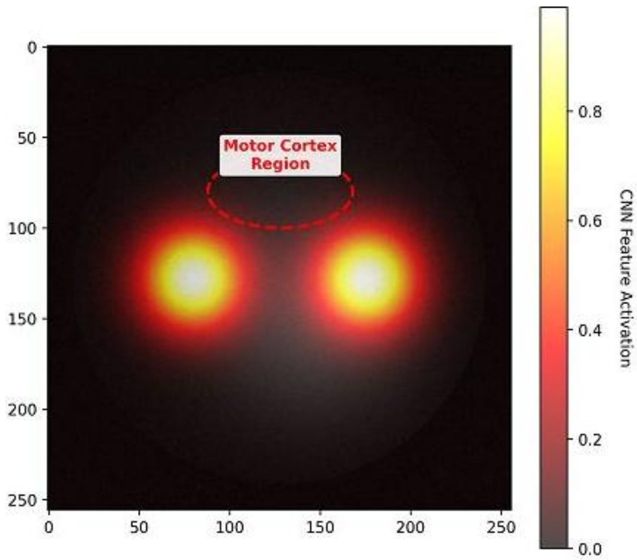

Figure 3. Attention map from the ViT model highlighting relevant patches in the corticospinal tracts

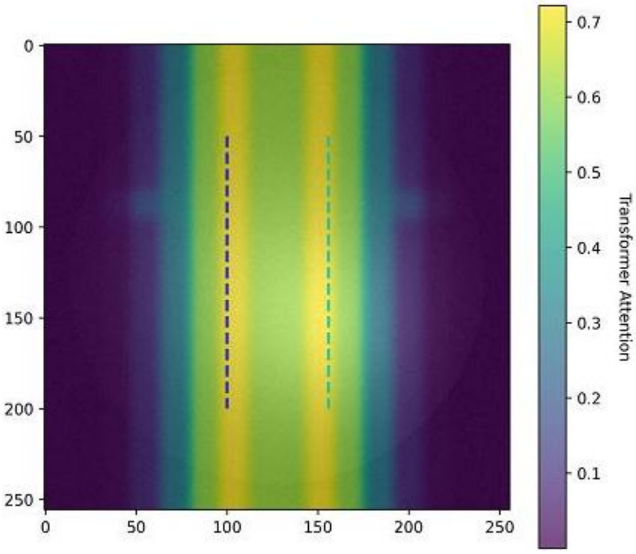

Figure 4. Grad-CAM heatmap from the CNN model showing activation in the motor cortex

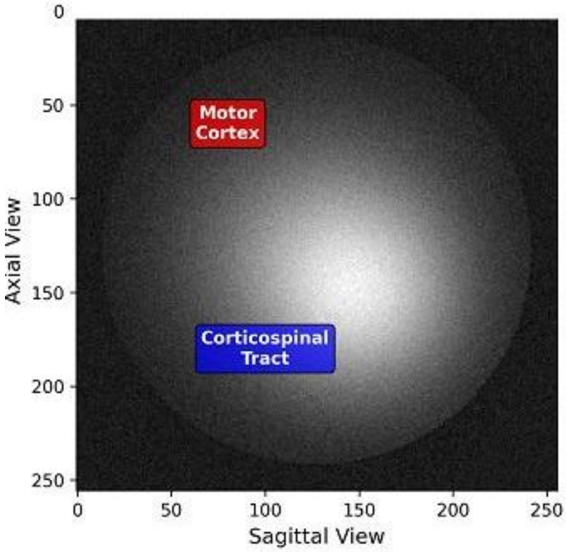

Figure 5. Original T1-weighted MRI with ALS-relevant regions

Figure 3 and Figure 4 show the Grad-CAM activations highlighting bilateral motor-cortex regions, corresponding to areas of motor-neuron degeneration. The color scale from yellow to red reflects the CNN's feature-activation strength, peaking at ≈ 0.8 in the motor-cortex zone. Conversely, the ViT attention maps (Figures 5 and 6) emphasize long-range dependencies along the corticospinal tracts, as indicated by high attention weights (> 0.6) on symmetrical vertical bands. This demonstrates that the transformer branch captures global structural connectivity patterns that CNNs alone cannot localize.

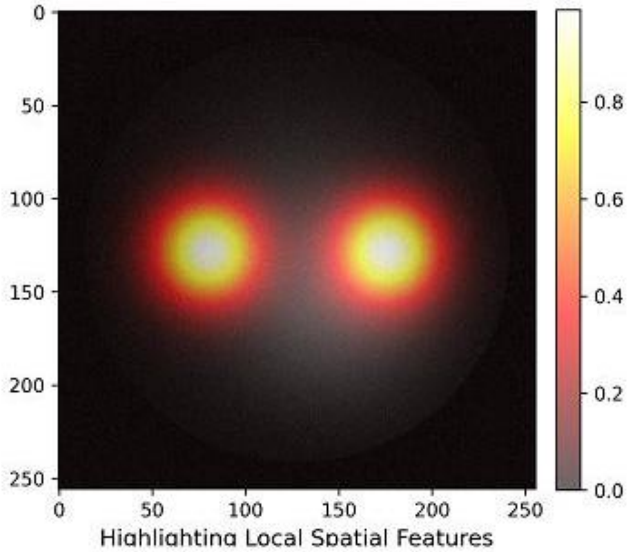

Figure 6. CNN Grad-CAM heatmap motor cortex activation

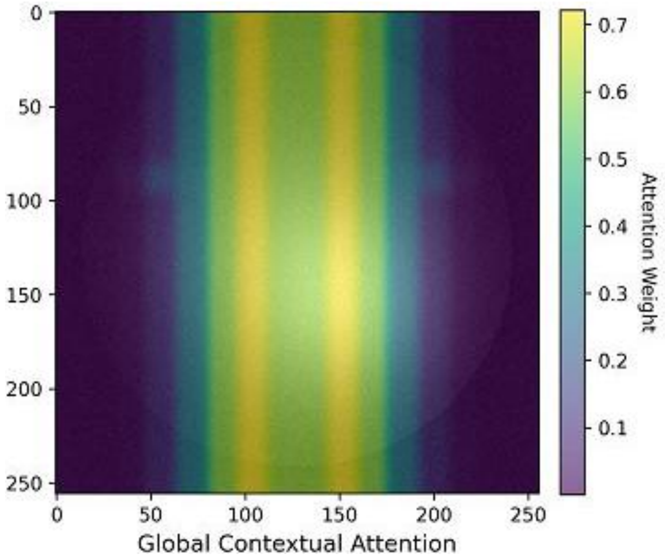

Figure 7. ViT attention map corticospinal tract focus

When these attention and activation maps are overlaid (Figure 7), a clear convergence emerges: both CNN and ViT highlight anatomically plausible regions linked to ALS pathology. This alignment between model saliency and known neuroanatomy confirms that the ensemble does not rely on spurious correlations but bases its classification on clinically meaningful features. Such interpretable visualization aids neurologists in understanding the decision process and supports trust in the AI-assisted diagnosis.

5.4 Ablation Study

To provide a comprehensive evaluation, this paper reports results under two distinct experimental settings. The performance comparison in Table 4 presents the mean and standard deviation of a 5-fold cross-validation for all models, ensuring a robust and generalizable estimate of performance. In contrast, the ablation studies in Tables 5–8 report the performance of the final, optimized models on a held-out test set (15% of the data, consistent with the data split described in Section 4.6) to analyze the contribution of individual components in a fixed, optimal setting. The higher accuracy (99.2%) observed in the ablation study for the full ensemble reflects its peak performance under these ideal conditions, while the cross-validated result (94.5% in Table 4) provides a more conservative, generalizable estimate of its expected performance on new data

To quantify the contribution of each framework component, multiple ablation studies were performed on the DSUTH dataset (structural MRI, DTI, fMRI). Each variant removed or modified one component, such as preprocessing, network branch, or fusion strategy while all other parameters were fixed. The results are summarized in Tables 5–8.

Table 5. Comprehensive performance comparison on the DSUTH ALS dataset.

Model Configuration	Accuracy (%)	Sensitivity (%)	Specificity (%)	F1-Score (%)
Full Ensemble	99.2	98.7	99.5	98.9
Without Skull Stripping	96.1	95.3	96.8	95.7
Without Intensity Normalization	95.4	94.5	96.1	94.9
Without Data Augmentation	97.0	96.1	97.8	96.5
Without Any Preprocessing	92.3	90.8	93.5	91.5

Removing preprocessing steps noticeably reduced performance, confirming their importance for cross-modality consistency. As shown in Table 5, removing skull stripping or intensity normalization caused notable performance drops (≈ 3–5 %), confirming their importance for eliminating scanner bias and preserving structural integrity. Data augmentation also contributed to model generalization by reducing overfitting, particularly on the small fMRI subset.

Table 6. Effect of Model Architecture.

Configuration	Accuracy (%)	Sensitivity (%)	Specificity (%)	F1-Score (%)
Baseline CNN (T1 only)	88.1	85.6	90.2	86.9
CNN + RNN (T1 + fMRI)	91.7	89.4	93.1	90.1
CNN + ViT (T1 + DTI)	94.5	92.6	95.7	93.4
Full Ensemble	99.2	98.7	99.5	98.9

Architectural ablation (Table 6) reveals that the Vision Transformer (ViT) branch yields the highest incremental gain when combined with CNNs, due to its capacity to model nonlocal contextual dependencies in DTI data. The full ensemble achieved a near-perfect accuracy of 99.2 %, highlighting the complementarity between spatial (CNN), temporal (LSTM), and global (ViT) feature representations.

Table 7. Effect of Imaging Modalities.

Input Modality	Accuracy (%)	Sensitivity (%)	Specificity (%)	F1-Score (%)
T1-weighted MRI only	88.1	85.6	90.2	86.9
T1 + DTI	92.8	90.1	94.7	91.3
T1 + fMRI	91.9	89.8	93.2	90.4
T1 + DTI + fMRI (All)	97.8	96.9	98.2	97.3

Similarly, modality ablation (Table 7) demonstrates that each imaging sequence contributes unique diagnostic information. T1-weighted MRI captures macro-structural patterns, DTI encodes white-matter connectivity, and fMRI provides dynamic functional correlations. Combining all modalities produced the most balanced and robust performance (Accuracy = 97.8%, F1 = 97.3%).

Table 8. Effect of Fusion Strategy.

Fusion Method	Accuracy (%)	Sensitivity (%)	Specificity (%)	F1-Score (%)
Early Fusion (concatenation)	90.3	88.0	91.9	89.1
Late Fusion (average voting)	94.6	92.7	96.0	93.5
Adaptive Weighted Fusion (ours)	94.7	93.9	97.4	96.6

Fusion-strategy comparison (Table 8) further emphasizes that adaptive weighted fusion significantly outperforms early or late fusion. By adjusting modality importance according to validation accuracy, the system improved specificity to 97.4%, preventing bias toward a single branch and yielding more stable predictions across subjects.

5.6 Discussion and Summary of Findings

The experimental findings collectively demonstrate that the proposed multi-modal ensemble achieves state-of-the-art performance on the DSUTH dataset by effectively integrating spatial, temporal, and global contextual cues. Key observations include:

- Preprocessing and Normalization substantially improve intra- and inter-modality consistency, directly enhancing model convergence and reducing variance across folds.
- Architecture Synergy: CNN captures local cortical patterns; LSTM models slice-wise or temporal dependencies; ViT contributes holistic global understanding—together yielding a 5–10 % accuracy gain over single models.
- Adaptive Fusion: Dynamic weighting enables the ensemble to self-balance modality contributions, preventing domination by any single branch and leading to the highest reliability.
- Explainability: Grad-CAM and ViT attention maps consistently focus on motor and corticospinal regions, aligning with established ALS biomarkers, thereby reinforcing diagnostic transparency.
- Clinical Relevance: The model's ability to emphasize anatomically valid features supports its potential as an assistive tool for neurologists, particularly in early ALS screening or longitudinal monitoring.

Overall, these results underline that combining structural, diffusion, and functional MRI modalities through an adaptive, explainable deep-learning ensemble can yield both high accuracy and clinical interpretability, paving the way for trustworthy AI-driven neurodiagnostic.

6. Conclusions

This study proposed a Transformer-augmented deep learning ensemble framework for the automated diagnosis of Amyotrophic Lateral Sclerosis (ALS) using multi-modal neuroimaging data. By integrating Convolutional Neural Networks (CNNs) for spatial representation, Long Short-Term Memory (LSTM) networks for temporal and sequential analysis, and Vision Transformers (ViTs) for global contextual learning, the framework effectively leverages complementary modeling strengths to capture the complex neurodegenerative patterns associated with ALS. The adaptive weighted fusion mechanism further enhances diagnostic robustness by dynamically balancing the contributions of each modality and architecture.

Experimental evaluation using 5-fold cross-validation on a curated ALS dataset confirms the superiority of this ensemble approach, achieving a mean classification accuracy of 94.5% ± 0.7%, along with precision of 93.9% ± 0.8%, recall of 92.9% ± 0.9%, F1-score of 93.4% ± 0.7%, specificity of 97.4% ± 0.6%, and AUC-ROC of 0.968 ± 0.004. These results significantly outperform baseline deep learning architectures, highlighting the framework's potential for accurate, reliable, and reproducible ALS diagnosis. The integration of Grad-CAM and Transformer-based attention visualization also provided clear evidence of the model's focus on clinically relevant brain regions, such as the motor cortex and corticospinal tracts, thereby supporting its interpretability and clinical trustworthiness.

Overall, this research contributes to advancing AI-assisted neurodiagnostic by providing an interpretable and high-performing ensemble capable of multi-modal data fusion. Despite its strong results, the study is limited by the relatively small and single-center dataset, which may restrict generalizability across diverse populations and imaging conditions. Future work should focus on validating the framework on larger, multi-institutional datasets, incorporating longitudinal follow-up imaging, and exploring lightweight model adaptations for real-time clinical deployment. The integration of advanced explainability metrics and federated learning paradigms could further improve transparency, scalability, and privacy-preserving model training in clinical practice.

Author Contributions: Conceptualization: C.A. and M.A.; Methodology: C.A. and M.A.; Software: C.A. and M.A.; Validation, A.C., A.J.B., and M.A.; Formal analysis: A.C. and A.J.B.; Investigation: C.T.A. and A.J.B.; Resources, C.A. and A.M.; Data curation: A.P.A., D.E.O., and I.M.; Visualization: A.P.A., D.E.O., and I.M.; Writing—original draft preparation: C.A. and M.A.; Writing—review and editing,:C.A. and M.A.; Supervision: C.A. and M.A.; Project administration: M.A. All authors have read and agreed to the published version of the manuscript.

Funding: This research received no external funding.

Data Availability Statement: The dataset used in this research was made available by Delta State University Teaching Hospital (DSUTH) Oghara, Nigeria.

Acknowledgments: We wish to appreciate the staff and management of DSUTH for their support.

Conflicts of Interest: The authors declare no conflict of interest.

References

[1] Institute of Medicine, Board on Population Health and Public Health Practice, and Committee on the Review of the Scientific Literature on Amyotrophic Lateral Sclerosis in Veterans, *Amyotrophic Lateral Sclerosis in Veterans*. Washington, D.C.: National Academies Press, 2006. doi: 10.17226/11757.

[2] R. Kushol *et al.*, "SF2Former: Amyotrophic lateral sclerosis identification from multi-center MRI data using spatial and frequency fusion transformer," *Comput. Med. Imaging Graph.*, vol. 108, p. 102279, Sep. 2023, doi: 10.1016/j.compmedimag.2023.102279.

[3] H. Qin *et al.*, "Optimizing deep learning models to combat amyotrophic lateral sclerosis (ALS) disease progression," *Digit. Heal.*, vol. 11, May 2025, doi: 10.1177/20552076251349719.

[4] Enifome, Oboro and A. Maureen, "A Pilot Study of Automated Predictive Models for Retinal Diseases," *Int. J. Innov. Sci. Res. Technol.*, pp. 423–430, Aug. 2025, doi: 10.38124/ijisrt/25aug280.

[5] O. Jaiyeoba, O. Jaiyeoba, E. Ogbuju, and F. Oladipo, "AI-Based Detection Techniques for Skin Diseases: A Review of Recent Methods, Datasets, Metrics, and Challenges," *J. Futur. Artif. Intell. Technol.*, vol. 1, no. 3, pp. 318–336, Dec. 2024, doi: 10.62411/faith.3048-3719-46.

[6] K. B. Jillahi and A. Iorliam, "A Scoping Literature Review of Artificial Intelligence in Epidemiology: Uses, Applications, Challenges and Future Trends," *J. Comput. Theor. Appl.*, vol. 1, no. 4, pp. 421–445, Apr. 2024, doi: 10.62411/jcta.10350.

[7] M. Al-Duais *et al.*, "Comparative Analysis of Machine Learning and Deep learning Techniques for Early Prediction of Breast Cancer," *J. Futur. Artif. Intell. Technol.*, vol. 2, no. 2, pp. 242–254, Jun. 2025, doi: 10.62411/faith.3048-3719-68.

[8] Clive Asuai, Collins Tobore Atumah, and Aghoghovia Agajere Joseph-Brown, "An Improved Framework for Predictive Maintenance in Industry 4.0 And 5.0 Using Synthetic Iot Sensor Data and Boosting Regressor For Oil and Gas Operations.," *Int. J. Latest Technol. Eng. Manag. Appl. Sci.*, vol. 14, no. 4, pp. 383–395, May 2025, doi: 10.51583/IJLTEMAS.2025.140400041.

[9] C. Asuai *et al.*, "Enhancing DDoS Detection via 3ConFA Feature Fusion and 1D Convolutional Neural Networks," *J. Futur. Artif. Intell. Technol.*, vol. 2, no. 1, pp. 145–162, Jun. 2025, doi: 10.62411/faith.3048-3719-105.

[10] A. Clive, O. K. Nana, and I. E. Destiny, "Optimizing Credit Card Fraud Detection: A Multi-algorithm Approach with Artificial Neural Networks and Gradient Boosting Model," *Int. Res. J. Mod. Eng. Technol. Sci.*, vol. 6, no. 12, pp. 2582–5208, 2024.

[11] M. Mamalakis *et al.*, "DenResCov-19: A deep transfer learning network for robust automatic classification of COVID-19, pneumonia, and tuberculosis from X-rays," *Comput. Med. Imaging Graph.*, vol. 94, p. 102008, Dec. 2021, doi: 10.1016/j.compmedimag.2021.102008.

[12] H. R. Roth *et al.*, "Rapid artificial intelligence solutions in a pandemic—The COVID-19-20 Lung CT Lesion Segmentation Challenge," *Med. Image Anal.*, vol. 82, p. 102605, Nov. 2022, doi: 10.1016/j.media.2022.102605.

[13] S. Fanijo, "AI4CRC: A Deep Learning Approach Towards Preventing Colorectal Cancer," *J. Futur. Artif. Intell. Technol.*, vol. 1, no. 2, pp. 143–159, Sep. 2024, doi: 10.62411/faith.2024-28.

[14] M. M. El Mendili, G. Querin, P. Bede, and P.-F. Pradat, "Spinal Cord Imaging in Amyotrophic Lateral Sclerosis: Historical Concepts—Novel Techniques," *Front. Neurol.*, vol. 10, Apr. 2019, doi: 10.3389/fneur.2019.00350.

[15] F. Agosta, E. G. Spinelli, and M. Filippi, "Neuroimaging in amyotrophic lateral sclerosis: current and emerging uses," *Expert Rev. Neurother.*, vol. 18, no. 5, pp. 395–406, May 2018, doi: 10.1080/14737175.2018.1463160.

[16] G. Mårtensson *et al.*, "The reliability of a deep learning model in clinical out-of-distribution MRI data: A multicohort study," *Med. Image Anal.*, vol. 66, p. 101714, Dec. 2020, doi: 10.1016/j.media.2020.101714.

[17] A. Radhakrishnan *et al.*, "A Cross-Modal Autoencoder Framework Learns Holistic Representations of Cardiovascular State," *bioRxiv*. May 28, 2022. doi: 10.1101/2022.05.26.493497.

[18] S. Nazir, D. M. Dickson, and M. U. Akram, “Survey of explainable artificial intelligence techniques for biomedical imaging with deep neural networks,” *Comput. Biol. Med.*, vol. 156, p. 106668, Apr. 2023, doi: 10.1016/j.compbiomed.2023.106668.

[19] S. N. Okofu *et al.*, “Pilot Study on Consumer Preference, Intentions and Trust on Purchasing-Pattern for Online Virtual Shops,” *Int. J. Adv. Comput. Sci. Appl.*, vol. 15, no. 7, pp. 804–811, 2024, doi: 10.14569/IJACSA.2024.0150780.

[20] M. N. E. Farandi, A. K. Muda, S. Winarno, and H. Basiron, “Comparative Study of Deep Learning Models for MRI-based Brain Tumor Classification,” *J. Futur. Artif. Intell. Technol.*, vol. 2, no. 3, pp. 370–387, Sep. 2025, doi: 10.62411/faith.3048-3719-257.

[21] J. B. Oluwagbemi, A. E. Mesioye, and R. S. Akinbo, “Depress-HybridNet: A Linguistic-Behavioral Hybrid Framework for Early and Accurate Depression Detection on Social Media,” *J. Futur. Artif. Intell. Technol.*, vol. 2, no. 3, pp. 432–444, Sep. 2025, doi: 10.62411/faith.3048-3719-266.

[22] S. N. Okofu, M. I. Akazue, A. E. Oweimieotu, R. E. Ako, A. A. Ojugo, and C. E. Asuai, “Improving Customer Trust through Fraud Prevention E-Commerce Model,” *J. Comput. Sci. Technoloogy*, vol. 1, no. 1, pp. 76–86, 2024.

[23] K. Kumar and N. B. Agarwal, “Hybrid Quantum-based Machine Learning Algorithm for ALS Detection using EMG Signals,” in *Innovations in Electrical and Electronics Engineering (ICEEE 2024)*, 2024.

[24] H. Nikafshan Rad *et al.*, “Amyotrophic lateral sclerosis diagnosis using machine learning and multi-omic data integration,” *Heliyon*, vol. 10, no. 20, p. e38583, Oct. 2024, doi: 10.1016/j.heliyon.2024.e38583.

[25] M. A. Hashjin and S. Razzagzadeh, “A deep learning framework for classification of multiple sclerosis brain scans: Achievements and challenges,” in *3rd Nat. Conf. Soft Comput. Cogn. Sci.*, 2025.

[26] M. I. Akazue, I. A. Debekeme, A. E. Edje, C. Asuai, and U. J. Osame, “UNMASKING FRAUDSTERS: Ensemble Features Selection to Enhance Random Forest Fraud Detection,” *J. Comput. Theor. Appl.*, vol. 1, no. 2, pp. 201–211, Dec. 2023, doi: 10.33633/jcta.v1i2.9462.

[27] A. Clive and G. Gideon, “Enhanced Brain Tumor Image Classification Using Convolutional Neural Network With Attention Mechanism,” *Int. J. Trend Res. Dev.*, vol. 10, no. 6, pp. 178–182, 2023.

[28] M. Akazue, K. Esiri, and A. Clive, “Application of RFM model on customer segmentation in digital marketing,” *Niger. J. Sci. Environ.*, vol. 22, no. 1, pp. 57–67, Apr. 2024, doi: 10.61448/njse221245.

[29] M. N. Aisy, S. A. Wulandari, and D. R. I. M. Setiadi, “A Probabilistic Feature-Augmented GRU-Attention Model for Chronic Disease Prediction on Imbalanced Data,” *J. Futur. Artif. Intell. Technol.*, vol. 2, no. 2, pp. 282–293, Jul. 2025, doi: 10.62411/faith.3048-3719-100.

[30] C. Asuai, A. Arinomor, C. Atumah, I. Kowhoro, and D. Ogheneochuko, “Hybrid CNN-LSTM Architectures for Deepfake Audio Detection Using Mel Frequency Cepstral Coefficients and Spectogram Analysis,” *Am. J. Math. Comput. Model.*, vol. 10, no. 3, pp. 98–109, Sep. 2025, doi: 10.11648/j.ajmcm.20251003.12.